Received: 26 April 2023 | Accepted: 31 August 2023

DOI: 10.1002/jpln.202300142

RESEARCH ARTICLE

Organic matter type and soil texture shape prokaryotic communities during early-stage soil structure formation

Tongyan Yao[1] | **Franziska Bucka**[2] | **Ingrid Kögel-Knabner**[2,3] | **Claudia Knief**[1]

[1]Institute of Crop Science and Resource Conservation (INRES), Molecular Biology of the Rhizosphere, University of Bonn, Bonn, Germany

[2]Soil Science, Weihenstephan Department of Ecology and Ecosystem Management, TUM School of Life Sciences Weihenstephan, Technical University of Munich, Freising, Germany

[3]Institute for Advanced Study, Technical University of Munich, Garching, Germany

Correspondence
Claudia Knief, Institute of Crop Science and Resource Conservation (INRES), Molecular Biology of the Rhizosphere, University of Bonn, Nussallee 13, 53115 Bonn, Germany.
Email: knief@uni-bonn.de

This article has been edited by Kai Uwe Totsche.

Funding information
Deutsche Forschungsgemeinschaft, Grant/Award Number: 276973576

Abstract

Background: Organic matter (OM) serves as substrate for heterotrophic microbial growth. Soil structure supports microbial life by providing various niches for colonization. Microorganisms in turn contribute to soil structure formation.

Aims: We aim to understand how OM of different origin and soil texture affect prokaryotic community structure and the implications on early-stage soil structure formation.

Methods: An artificial soil incubation experiment was conducted with different types of OM, including bacterial necromass and particulate organic matter (POM) of larger or smaller size (sPOM). The mineral composition was modified to obtain a clay loam, loam, and sandy loam texture. The abundance and composition of a natural microbial inoculum were determined after 30 days of incubation by real-time PCR and 16S rRNA gene sequencing, respectively.

Results: The different OM types had a stronger effect on the prokaryotic community structure and abundance than texture. The necromass treatment supported the most distinct prokaryotic community with the highest abundance and lowest diversity, as well as the most intense formation of water-stable microaggregates in comparison to POM and sPOM treatments. Abundant bacterial taxa in all treatments are known to include extracellular polymeric substance producers, indicating that functional redundancy warrants aggregation by gluing agents. Texture-related effects were most consistent in the POM treatment, where larger prokaryotic populations were observed in the coarser-textured soils with fewer but larger soil pores and lower soil water content.

Conclusions: Differences in prokaryotic community structure and abundance due to OM source indicate that aggregation is dependent on different ecological strategists, a POM-degrading population that promotes aggregation and contributes to necromass formation, and a necromass-degrading consortium in which bacteria play a major role.

KEYWORDS
aggregate formation, artificial soil, organic matter, prokaryotic community, soil texture

1 | INTRODUCTION

Soil is a porous and heterogeneous material covering a large surface area on Earth and supporting microscopic and macroscopic lives. It consists of a solid phase with minerals and organic matter (OM) of varying sizes, as well as a liquid and a gas phase. The solid and liquid phases of the soil form its structure, providing soil microorganisms with highly heterogeneous habitats. The fine mineral particles are categorized into three size classes, that is, sand, silt, and clay, and their proportion defines soil texture. Previous studies reported that the prokaryotic community structure and abundance can be affected by soil texture, especially by soil clay content (Biesgen et al., 2020; Obayomi et al., 2021).

Soil texture is inherently linked to soil structure, which is one of the most important properties of soil, regulating diverse soil functions such as ventilation, nutrient accessibility, carbon sequestration, and soil life (Bronick & Lal, 2005). It refers to the arrangement of heterogeneously composed soil particles of varying sizes, which are called aggregates (Oades & Waters, 1991; Totsche et al., 2018). As a key component of soil structure, soil aggregation plays an important role in the development of bacterial communities (Rillig et al., 2017). Considering the inherent linkage between soil texture and soil structure, it remains unclear to what extent the prokaryotic community structure responds to soil texture during soil structure formation by aggregation processes. In turn, bacterial cells support soil aggregation by directly adhering with their cell walls to soil mineral surfaces (Krause et al., 2019; Miltner et al., 2009). Moreover, bacteria secrete gluing agents such as extracellular polymeric substances (EPSs) and mucilage. These gluing agents participate in the aggregation of building units to soil aggregates, thus initiating and improving soil aggregation (Amelung et al., 2023; Costa et al., 2018; Huang et al., 2005; Totsche et al., 2018).

While soil aggregation offers bacteria the physical structure of their habitats, soil organic matter (SOM) is the most critical chemical component. SOM was initially thought to consist predominantly of plant litter, but studies in the recent decade have documented the unneglectable contribution of microbial necromass, accounting for up to half of the SOM in diverse terrestrial ecosystems (Liang et al., 2019). In addition to studies emphasizing the importance of microbial necromass in the soil C pool, research has been conducted to understand the recycling, stabilization, and destabilization of microbial necromass in soil (Buckeridge et al., 2022; Wang et al., 2020) and to reveal the underlying mechanisms of decomposition of respective components in microbial necromass (Hu et al., 2020). Moreover, OM is important for the formation and stabilization of soil aggregates (Lehndorff et al., 2021; Oades & Waters, 1991), which in turn is affected by the metabolic activity of microorganisms. However, little is known about the difference in decomposition between the "traditional" SOM source, plant debris, and microbial necromass. To understand this difference, a comparison of microbial community development in dependence on these two types of organic carbon (OC) sources can provide valuable insight. Besides the type of OM, the size of OM particles plays a role in soil aggregation (Bucka et al., 2021), which may likewise have effects on microbial community development.

With the aim to study effects of texture as well as OM type and size on the prokaryotic community development during initial stages of soil aggregation, we conducted an artificial soil aggregation experiment. This included setups with three different textures in combination with three OM treatments, varying in OM type and size, and a control without OM. After incubation for 30 days, we analyzed the prokaryotic abundance and community composition by quantitative PCR (qPCR) and 16S rRNA gene amplicon sequencing, respectively. We hypothesized that during early aggregation, (1) both texture and OM type have significant effects on the abundance and composition of prokaryotic communities, (2) with OM type (necromass vs. particulate organic matter [POM]) as well as OM size (POM vs. small particulate organic matter [sPOM]) influencing prokaryotic communities. (3) These differences in community development in turn have implications for soil structure development.

2 | MATERIALS AND METHODS

2.1 | Artificial soil experiment

The artificial soil experiment with different soil textures and different OM treatments was performed by Bucka et al. (2021). Artificial soil mixtures with different mineral composition were defined to represent three common soil textures, clay loam, loam and sandy loam. The detailed composition of the mineral mixtures is described in Bucka et al. (2019). Briefly, 89% of quartz grains in the size of clay, silt, and sand were used at different ratios to obtain the three textures. In addition, 7% illite, 3% montmorillonite, and 1% goethite were added to imitate the reactive surfaces of soils.

Besides different soil textures, four OM treatments were implemented. These included bacterial necromass (referred to as "necromass"), POM, sPOM, and a control treatment without OM addition. The bacterial necromass consisted of gamma radiation-sterilized *Bacillus subtilis* biomass. The POM and sPOM materials were added as milled hay litter. The hay litter was grass–clover hay, dry-sieved to two size classes, 0.63–2 mm (POM) and <63 μm (sPOM). All three OM materials were applied with the same OC concentration (13 mg OC/g in the final mixture).

To provide the artificial soil with an initial microbial community, an inoculum extracted with water from an arable Cambisol was added to each microcosm (Lehmann et al., 2007; Pronk et al., 2012). Each microcosm contained 300 g of the mixture including the OM materials. Totally, 36 microcosms (3 textures × 4 treatments × 3 replicates) were incubated with a constant water tension of −15 kPa on a suction plate in the dark for 30 days at 20°C as described in Bucka et al. (2021). After incubation, the mixtures were destructively sampled and samples were frozen at −20°C until further analyses.

2.2 | DNA extraction

Genomic DNA was extracted from 0.25 g of frozen artificial soil sample using the NucleoSpin Soil DNA extraction kit (Macherey-Nagel) according to the manufacturer's instructions with the following adjustment: each artificial soil sample was resuspended in 700 µL of SL1 buffer and 150 µL of SX enhancer, mechanical cell lysis was performed with a FastPrep−96 homogenizer (MP Biomedicals) at 1800 oscillations/min for 1 min, and the extracted DNA was finally eluted with 50 µL of PCR-grade water (55°C) twice. The extracted DNA was stored at −20°C until further use.

2.3 | qPCR of the 16S rRNA gene

To estimate the abundance of prokaryotes in the inoculum and the artificial soil samples, qPCR of the V4–V5 region of the 16S rRNA gene with a universal primer set 515f/806r was performed on a CFX96 real-time PCR detection system (BioRad), essentially as described by Frindte et al. (2020). Different from it, undiluted DNA extracts were used in the qPCR assays, as tests with different dilutions revealed no inhibition of the undiluted DNA extracts.

2.4 | PCR amplification of the 16S rRNA gene and amplicon sequencing

PCR products for sequencing were generated with primer set 515f/806r following a two-step PCR protocol. For the first step, PCR reactions were performed in a 20-µL assay, containing 0.1 µM of each primer, 1 U Herculase Fusion DNA Polymerase (Agilent Technologies), 1× Herculase II reaction buffer, 250 mM of each dNTP, 2 mM $MgCl_2$, 0.8 µg/µL BSA, and 1 µL of template DNA. The PCR for each sample was performed in triplicates. The reactions were started with an initial denaturation at 95°C for 2 min, followed by 25 cycles of denaturation at 95°C for 20 s, annealing at 52°C for 20 s, and elongation at 72°C for 30 s, and ended with a final elongation at 72°C for 10 min. Triplicates for each sample were then mixed and used as template DNA in a second PCR to add sample-specific barcodes to the PCR products. For this second PCR, reactions were conducted in 50-µL assays, containing 0.1 µM of a specifically barcoded 515f primer (Frindte et al., 2019), 0.1 µM of primer 806r, 1 U Herculase Fusion DNA Polymerase (Agilent Technologies), 1× Herculase II reaction buffer, 250 mM of each dNTP, 1.5 mM $MgCl_2$, 0.8 µg/µL BSA, and 3 µL of template DNA. The thermal cycling protocol for the second PCR was the same as for the first PCR, but consisted of only six cycles.

The DNA concentration of the PCR products was determined by the Qubit 2.0 dsDNA HS Assay on the Qubit 2.0 Fluorometer (Thermo Fisher Scientific), following the manufacturer's instructions. Afterward, the PCR products were pooled at equal concentrations and purified with 20% PEG solution (20% [w/v] PEG 8000, 2.5 M NaCl). The mixtures were forwarded to the West German Genome Center (at the University of Bonn) for library preparation and sequencing on a Miseq sequencing platform (Illumina) to generate 2 × 300 bp reads.

Raw sequence data were firstly demultiplexed using Cutadapt (2.10). Sequence data were processed in QIIME2 according to the published tutorials (Bolyen et al., 2019). Briefly, the demultiplexed sequence data were imported into QIIME2 as a manifest file. The manifest was first denoised with dada2, including removal of noisy sequences, chimeras, and singletons and correction of errors in marginal sequences. In this step, the sequence data of the control treatment without OM addition and the inoculum were excluded because they contained only a few reads of low quality, resulting from the small prokaryotic population size in these samples. The classification of taxa at amplicon sequence variant (ASV) level was conducted using the classify-sklearn classifier against the SILVA 138 database. A phylogenetic tree was then built. Sequences assigned to chloroplasts and mitochondria were removed from the final ASV table. Finally, the feature table, taxonomic information, and a phylogenetic tree were exported to R for further analysis.

We obtained 2,300,399 high-quality sequences for all samples except the controls, and between 9613 and 130,478 sequences per sample. All samples were rarefied to 9613 sequences per sample to calculate the alpha diversity indexes, determine beta diversity, and analyze the prokaryotic genera responding to treatments.

2.5 | Calculations and statistical analyses

The 16S rRNA gene copy number for the inoculum and each soil sample estimated by qPCR was directly calculated by the CFX Manager software and then normalized to gene copy numbers per gram dry soil. The homogeneity of variances was checked by Levene's test. Normality of the residuals was checked by the Shapiro–Wilk test. Two-way analysis of variance (ANOVA) followed by a post hoc Tukey HSD test was performed to evaluate the effects of OM type and soil texture on the abundance of prokaryotes. All tests were done using the package "*car*" in R.

Alpha diversity indices, including observed ASVs, Chao1 index (Chao, 1984), Shannon index (Shannon, 1948), and Pielou's evenness (Pielou, 1966), were calculated in R. Significant differences in alpha diversity related to OM type and soil texture were evaluated by two-way ANOVA. Variation in beta diversity was evaluated in a nonmetric multidimensional scaling (NMDS) plot based on a Bray–Curtis dissimilarity matrix. To test for significant differences between groups of samples, permutational multivariate analysis of variance (PERMANOVA) was performed on Bray–Curtis distances, and the *p* values were corrected using the false discovery rate.

To identify genera that responded to the OM addition treatments, an analysis of compositions of microbiomes with bias correction (ANCOM-BC; Becker et al., 2022; Lin & Peddada, 2020) based on relative abundances was performed, which enables pair-wise comparisons of taxon abundance in different OM treatments. All parameters in ANCOM-BC were left default. Genera with a relative abundance lower than 0.1% in all OM treatments were excluded for this analy-

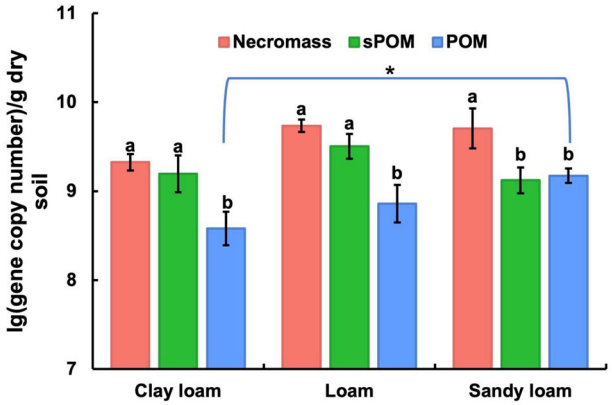

FIGURE 1 Prokaryotic 16S rRNA gene abundance in the artificial soil microcosms in dependence on OM type in different textured soil. Different letters denote significant differences among treatments according to post hoc tests following two-way ANOVA with $p < 0.05$ ($n = 3$). An asterisk denotes a significant difference between connected soil textures under the same OM treatment.

sis. Responsive genera with differences in relative abundance between the OM treatments were classified into five groups. These were three treatment groups where the relative abundance of genera in one treatment was significantly higher than in the other two treatments, one shared group where the three OM treatments had no significant difference on prokaryotic relative abundance, and a group containing the rest of the genera. The results were visualized in a ternary plot.

All calculations, statistics, and data visualizations were performed with R 4.1.1 or in Microsoft Excel 16.72. A significance level of $\alpha = 0.05$ was chosen for significance tests.

3 | RESULTS

3.1 | Prokaryotic abundance in the soil aggregation experiment

The mean 16S rRNA gene copy number that was determined in the inoculum was used to estimate the gene copy number in the microcosms at the beginning of the incubation, resulting in 1.3×10^5 gene copies per gram dry soil. After incubation, gene copy numbers were lowest in the control treatment without OM addition (1.2×10^5 gene copies) per gram dry soil; it was in the range of the qPCR detection limit and approximately 3×10^3- to 50×10^3-fold lower compared to the treatments with OM addition. This indicated that no population increase had taken place in the absence of OM during the incubation experiment, and the control treatment was excluded from the further qPCR data analysis.

Both the OM types and soil textures exerted a significant effect on the prokaryotic abundance in the artificial soils (two-way ANOVA on log-transformed data: OM types, $F = 29.8$, $p < 0.001$; soil texture, $F = 7.8$, $p < 0.01$; Figure 2). In addition, a significant interaction between OM type and soil texture was detected ($F = 3.1$, $p < 0.05$). Resolving the dataset by soil texture to evaluate the OM treatment effect in more detail revealed consistently a significantly higher prokaryotic abundance in treatments with necromass than with POM for all three textures. In case of sPOM, the prokaryotic abundance was equally high as observed in the presence of necromass in clay loam and loam soil, whereas it was similar to the lower abundance observed with POM in the sandy soil. Focusing on the effects of texture, the differences observed across textures (i.e., a slightly lower abundance of prokaryotes in clay loam compared to loam and sandy loam soil) were not well resolved within the different OM treatments. Only in the POM treatment, the prokaryotic abundance in the clay loam soil was significantly lower than in the sandy loam soil (ANOVA with post hoc tests, $p < 0.05$). A similar trend was seen in the necromass treatment.

Major differences in bacterial colonization were confirmed by fluorescence microscopy, which was applied to analyze surface colonization of individual particles from the loam texture microcosms. The highest population of prokaryotic cells was observed on the surface of soil particles from the necromass treatment, followed by the (s)POM treatments, while only very few cells were observed on particles from the control treatment (Figure S1).

3.2 | Prokaryotic community structure in dependence on OM type and texture

No high-quality sequences were obtained after sequence data processing for the inoculum and the control treatment without OM addition, also indicating a weak proliferation of the inoculated prokaryotic community without OM. Consequently, this treatment was again excluded from the further analyses. The high-quality sequences obtained for the other treatments were assigned to 18 phyla and 23 classes, primarily representing bacteria (> 95%). Among them, the average relative abundance of 11 classes was higher than 0.05%, including *Gammaproteobacteria* (35.9%), *Alphaproteobacteria* (25.3%), *Bacteroidia* (16.6%), *Bacilli* (14.4%), *Bdellovibrionia* (1.2%), *Polyangia* (0.5%), *Verrucomicrobiae* (0.5%), *Myxococcia* (0.3%), *Actinobacteria* (0.2%), *Babeliae* (0.1%), and *Fimbriimonadia* (0.1%) (Figure 3).

The alpha diversity of the communities was characterized by four indices—observed number of ASVs, Chao1 index, Shannon index, and Pielou's evenness (Figure 4). The three different soil textures had no significant effect on these indices (two-way ANOVA, $p > 0.05$; Figure 4B). On the contrary, the different OM types exerted clear effects on the diversity of the prokaryotic communities (two-way ANOVA, $p < 0.05$). An interaction between OM treatments and texture was not evident. The alpha diversity of the three OM treatments followed the order necromass < sPOM = POM, for observed ASVs, Chao1, and Shannon index (Figure 4A). The evenness index followed the same pattern, but differences were slightly less pronounced, being only significantly lower in the necromass treatment than in sPOM but not the POM treatment ($p < 0.05$).

Dissimilarities in the prokaryotic community composition were most evident in response to OM type, as depicted by the NMDS plot (Figure 5). The necromass samples clustered apart from the others and showed the tightest cluster, whereas the cluster of the POM treat-

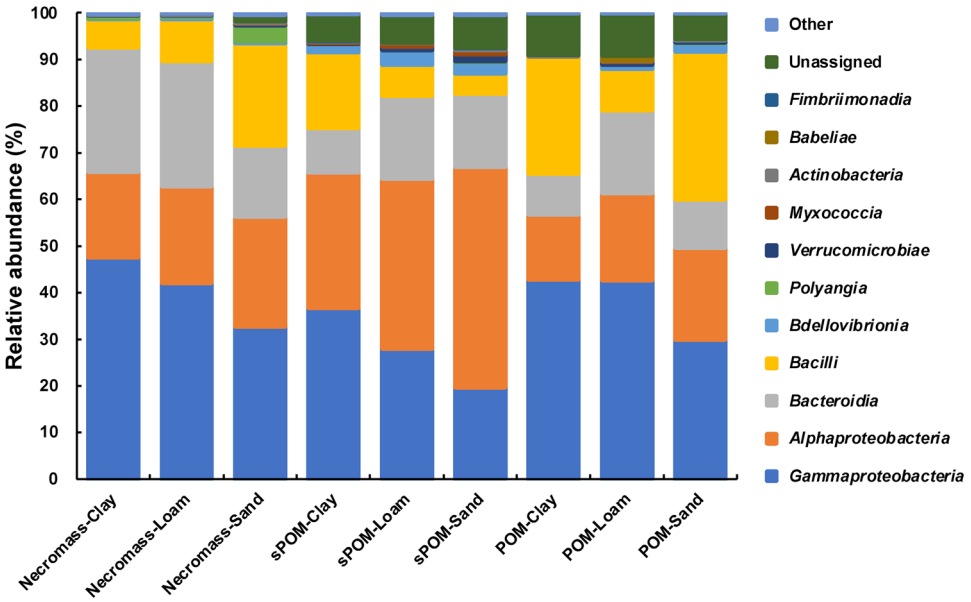

FIGURE 2 Prokaryotic community composition at the class level in the artificial soil microcosms in dependence on OM type and soil texture. Classes with a mean relative abundance below 0.05% were grouped as "other." "Clay" refers to the clay loam texture; "Sand" is short for sandy loam. Legend is sorted according to the appearance of taxa in the plot from bottom to top.

TABLE 1 Permutational multivariate analysis of variance (PERMANOVA) comparison of the prokaryotic community composition in the artificial soil microcosms in dependence on organic matter (OM) type and soil texture.

	F value	R^2	*p* value
OM treatment	10.0	0.40	0.001
Texture	2.1	0.09	0.013
OM treatment × texture	1.8	0.14	0.017
Pairwise comparisons of OM effects:			
Necromass vs. sPOM	13.1	0.45	0.0015
Necromass vs. POM	9.3	0.37	0.0015
sPOM vs. POM	3.1	0.16	0.0020
Specific evaluation of texture effects in:			
Necromass treatment	2.5	0.45	0.011
sPOM treatment	2.5	0.45	0.015
POM treatment	1.6	0.35	0.040

ment had an intersection with the sPOM treatment. Besides, the POM treatment formed the most dispersed cluster. Inside each cluster of the OM treatment, the samples seemed to be grouped by textures (Figure 5). The PERMANOVA results confirmed that the OM treatment exerted a significant effect on the prokaryotic community composition ($R^2 = 0.40$, $p = 0.001$; Table 1). Likewise, texture affected the community, though to lesser extent ($R^2 = 0.09$, $p = 0.013$), and part of the variation was explained jointly by OM treatment and texture effects.

A pair-wise comparison of dissimilarities between the OM treatments showed that all treatments were significantly different from each other (R^2 between 0.16 and 0.45, $p \leq 0.002$; Table 1). Due to the strong OM effect, we analyzed prokaryotic community responses to texture individually for each OM treatment. This revealed a significant influence of texture in all three OM treatments (R^2 between 0.35 and 0.45, $p < 0.05$; Table 1).

3.3 | Compositional differences of prokaryotic communities in dependence on OM type

As the prokaryotic community composition showed clear differences in dependence on the different OM treatments, the genera responding to different OM types were identified by ANCOM-BC. We focused on genera with a relative abundance of > 0.1% in at least one of the OM treatments; consequently, 75 out of 235 unique genera were selected. The highest number of specifically enriched taxa was found in the necromass treatment, followed by sPOM and then POM (Figure 5; Table 2). Thirteen genera were identified to be significantly enriched in the necromass treatment, accounting for 47.4% of the relative abundance in the necromass treatment and primarily representing *Bacteroidia*, *Alphaproteobacteria*, and *Gammaproteobacteria*. The most abundant genus was *Pedobacter* with a 4.9-fold enrichment over the sPOM and a 9.4-fold enrichment over the POM treatment. Less abundant but even more strongly enriched were an unclassified genus of *Yersiniaceae* and the genus *Luteimonas*. In the sPOM treatment, 11 genera were present at significantly higher relative abundance than in the necromass and POM treatment, but accounting for only 10.2% of the relative abundance in this treatment. Enrichment was strongest for different members of the *Bacteroidia* (*Pseudoflavitalea*, *Edaphobaculum*,

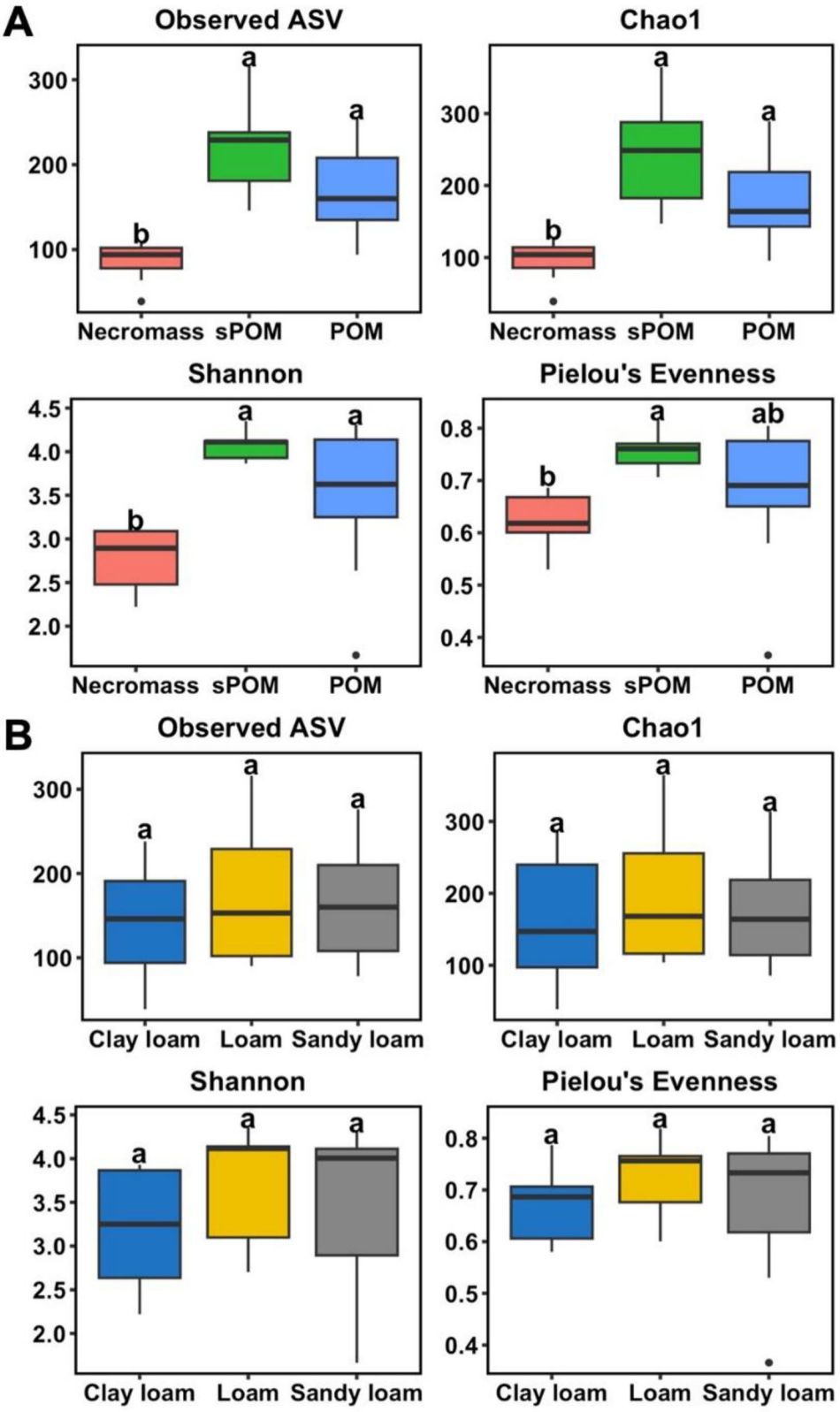

FIGURE 3 Alpha diversity of prokaryotic communities in artificial soil microcosms in dependence on OM type (A) and soil texture (B). Within each box, the black lines show median values; boxes extend from the first to the third quartile; the whiskers denote the most extreme values within the 1.5 interquartile range of the first and third quartile of each group; dots denote observations outside the range of the whiskers. Different letters indicate significant differences among treatments according to post hoc tests following two-way ANOVA with $p < 0.05$ ($n = 9$).

TABLE 2 Abundant genera (>0.1% relative abundance) with significant differences ($p < 0.05$) in relative abundance between OM treatments.

			Relative abundance (%)		
Group	**Class**	**Genus**	**Necromass**	**sPOM**	**POM**
Necromass	*Bacteroidia*	*Pedobacter*	20.41	4.18	2.17
	Alphaproteobacteria	*Sphingopyxis*	8.50	3.38	1.31
	Gammaproteobacteria	Unclassified_*Yersiniaceae*	8.21	0.02	0.02
	Gammaproteobacteria	*Achromobacter*	5.88	0.92	1.07
	Gammaproteobacteria	*Luteimonas*	1.59	0.00	0.02
	Alphaproteobacteria	*Devosia*	1.36	0.47	0.11
	Alphaproteobacteria	Unclassified_*Caulobacteraceae*	0.47	0.04	0.00
	Bacteroidia	*Parapedobacter*	0.24	0.00	0.00
	Gammaproteobacteria	*Herminiimonas*	0.19	0.00	0.00
	Bacteroidia	*Chryseobacterium*	0.15	0.00	0.00
	Bacteroidia	*Sphingobacterium*	0.14	0.00	0.00
	Actinobacteria	*Rhodococcus*	0.14	0.00	0.01
	Sumerlaeia	*Sumerlaea*	0.13	0.00	0.00
sPOM	*Alphaproteobacteria*	*Sphingobium*	0.00	3.09	0.98
	Bdellovibrionia	*Peredibacter*	0.33	2.06	0.65
	Bacteroidia	*Pseudoflavitalea*	0.08	1.81	0.20
	Bacteroidia	*Edaphobaculum*	0.08	1.33	0.21
	Bacteroidia	Unclassified_*Sphingobacteriaceae*	0.00	0.59	0.00
	Alphaproteobacteria	*Azospirillum*	0.00	0.37	0.00
	Myxococcia	Unclassified_*Myxococcaceae*	0.00	0.28	0.01
	Myxococcia	*Myxococcus*	0.00	0.28	0.06
	Gammaproteobacteria	Unclassified_*Enterobacterales*	0.00	0.17	0.00
	Fimbriimonadia	*Fimbriimonadaceae*	0.00	0.14	0.02
	Gammaproteobacteria	*Pseudorhodoferax*	0.00	0.11	0.01
POM	*Gammaproteobacteria*	*Duganella*	0.00	0.02	1.86
	Babeliae	*Vermiphilaceae*	0.00	0.00	0.34
	Bacteroidia	*Niastella*	0.00	0.09	0.33
	Alphaproteobacteria	Unclassified_*Paracaedibacteraceae*	0.00	0.00	0.12
	Gammaproteobacteria	Unclassified_*Methylophilaceae*	0.00	0.00	0.11
Other	*Gammaproteobacteria*	*Stenotrophomonas*	16.49^{a}	9.30^{ab}	3.81^{b}
	Alphaproteobacteria	*Brevundimonas*	6.21^{a}	6.34^{a}	1.42^{b}
	Alphaproteobacteria	*Allorhizobium–Neorhizobium–Pararhizobium–Rhizobium*	0.03^{b}	8.81^{a}	5.04^{a}
	Alphaproteobacteria	*Caulobacter*	1.53^{b}	8.42^{a}	3.81^{ab}
	Unclassified_bacteria	Unclassified_bacteria	0.47^{b}	5.84^{a}	7.08^{a}
	Gammaproteobacteria	*Massilia*	0.01^{b}	3.57^{a}	5.52^{a}
	Bacteroidia	*Chitinophaga*	0.43^{b}	1.73^{ab}	4.69^{a}
	Gammaproteobacteria	Unclassified_*Oxalobacteraceae*	0.06^{b}	2.64^{a}	2.92^{a}
	Gammaproteobacteria	*Pantoea*	0.00^{b}	0.22^{a}	4.23^{a}
	Gammaproteobacteria	*Cupriavidus*	0.00^{b}	0.58^{a}	2.48^{a}
	Gammaproteobacteria	*Pseudoxanthomonas*	0.02^{b}	2.35^{a}	0.09^{ab}
	Gammaproteobacteria	Unclassified_*Comamonadaceae*	0.07^{b}	0.88^{a}	1.49^{a}
	Bacteroidia	*Dyadobacter*	0.10^{b}	1.19^{a}	0.94^{ab}

(Continues)

TABLE 2 (Continued)

Group	Class	Genus	Relative abundance (%)		
			Necromass	sPOM	POM
	Alphaproteobacteria	*Novosphingobium*	0.59[a]	1.37[a]	0.16[b]
	Polyangia	*Pajaroellobacter*	1.40[a]	0.03[b]	0.03[ab]
	Gammaproteobacteria	*Variovorax*	0.07[b]	0.68[a]	0.62[ab]
	Alphaproteobacteria	Unclassified_*Xanthobacteraceae*	0.00[b]	0.45[a]	0.59[a]
	Bacteroidia	*Taibaiella*	0.02[b]	0.75[a]	0.23[ab]
	Unclassified_*Proteobacteria*	Unclassified_*Proteobacteria*	0.00[b]	0.28[a]	0.69[a]
	Bacteroidia	*Mucilaginibacter*	0.00[b]	0.48[a]	0.37[a]
	Alphaproteobacteria	Unclassified_*Alphaproteobacteria*	0.00[b]	0.77[a]	0.04[a]
	Verrucomicrobiae	*Chthoniobacter*	0.02[b]	0.65[a]	0.13[a]
	Gammaproteobacteria	*Janthinobacterium*	0.00[b]	0.17[a]	0.59[a]
	Bacteroidia	*Terrimonas*	0.00[b]	0.63[a]	0.07[a]
	Bacilli	*Terribacillus*	0.00[b]	0.14[a]	0.54[a]
	Bacilli	Unclassified_*Planococcaceae*	0.00[b]	0.23[a]	0.39[a]
	Alphaproteobacteria	*Phenylobacterium*	0.02[b]	0.26[a]	0.23[ab]
	Bdellovibrionia	*Bdellovibrio*	0.00[b]	0.22[a]	0.17[a]
	Gammaproteobacteria	*Methylotenera*	0.00[b]	0.11[a]	0.24[a]
	Gammaproteobacteria	*Polaromonas*	0.00[b]	0.19[a]	0.15[a]
	Bacteroidia	*NS11-12marinegroup*	0.00[b]	0.02[a]	0.20[a]
	Gammaproteobacteria	Unclassified_*Diplorickettsiaceae*	0.00[b]	0.14[a]	0.07[a]
	Alphaproteobacteria	Unclassified_*Caulobacteraceae*	0.00[b]	0.09[a]	0.10[a]
	Actinobacteria	*Nocardioides*	0.00[b]	0.15[a]	0.03[a]
	Gammaproteobacteria	*Herbaspirillum*	0.00[b]	0.04[a]	0.14[a]
	Alphaproteobacteria	*Mesorhizobium*	0.11[a]	0.03[a]	0.03[b]
	Bacilli	*Lysinibacillus*	0.00[b]	0.11[a]	0.04[a]
	Gammaproteobacteria	*Advenella*	0.00[b]	0.03[a]	0.11[a]
	Bacteroidia	*Spirosoma*	0.00[b]	0.01[a]	0.12[a]
	Gammaproteobacteria	*Hydrogenophaga*	0.00[a]	0.12[a]	0.00[b]
Shared	*Bacilli*	*Bacillus*	11.89	7.76	11.03
	Gammaproteobacteria	*Pseudomonas*	5.42	5.52	12.27
	Bacilli	*Weissella*	0.00	0.02	7.62
	Bacteroidia	*Flavobacterium*	1.23	0.99	2.63
	Alphaproteobacteria	Unclassified *Rhizobiaceae*	1.16	1.34	0.91
	Gammaproteobacteria	Unclassified *Enterobacteriaceae*	2.71	0.15	0.52

Note: The "Other" group includes genera with significant increase in relative abundance in two samples compared to the third one. The "Shared" group includes genera without significant differences in relative abundance among all three OM treatments. Different superscript letters denote significant differences in relative abundance among OM treatments in the "Other" group.

and an unclassified genus of *Sphingobacteriaceae*). Further genera that were detected represented different classes of bacteria. The POM treatment hosted the lowest number of specifically enriched genera, accounting for only 2.8% of the relative abundance. All five genera in POM were only of minor relative abundance in the other two OM types, mostly < 0.01%. The most abundant genus that was significantly enriched in POM was *Duganella*. Further 40 genera were shared in two OM treatments compared to a third one. Among these, 36 genera were shared by the sPOM and POM treatments and were less abundant in the necromass treatment, accounting for 40.3% of the mean relative abundance in all treatments. These genera were mainly members of the *Alphaproteobacteria*, *Gammaproteobacteria*, *Bacteroidia*, and *Bacilli*. Moreover, six genera were shared by the necromass and the sPOM treatments compared to the POM treatment, covering 17.6% of the mean relative abundance in all treatments, and seven genera were shared by the necromass and the POM treatments, accounting for

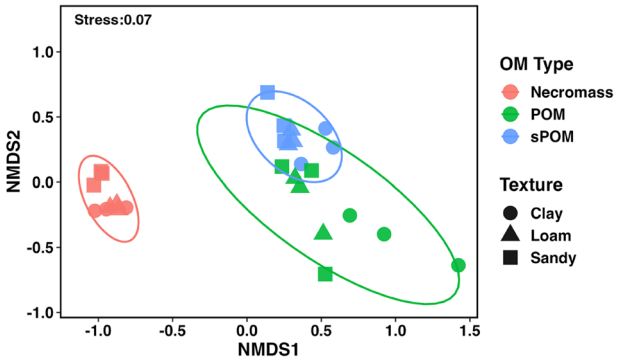

FIGURE 4 Nonmetric multidimensional scaling (NMDS) plot based on Bray–Curtis distances calculated for prokaryotic community composition between samples of the artificial soil microcosms in dependence on OM type and soil texture. Circles show the 95% confidence range of the OM treatments.

7.6% of the mean relative abundance in all treatments. Genera that were not significantly enriched in one or two OM treatments were primarily represented by *Bacillus*, *Pseudomonas*, *Weissella*, *Flavobacteria*, *Rhizobiaceae*, a genus of *Enterobacteriaceae*, *Sphingomonas*, and *Paenibacillus* (Table 2).

4 | DISCUSSIONS

4.1 | OM quality and size shape prokaryotic community structure and abundance during early aggregation

Prokaryotes in our artificial aggregation experiment proliferated by thousands to even tens of thousands in the OM addition treatments compared to the control without OM over the incubation period of 30 days (Figure 1). This shows that growth was strongly limited without OM addition, which is largely consistent with the findings of Bucka et al. (2021), who did not observe respiratory activity in this control treatment. Moreover, the absence of OM and the restricted prokaryotic growth strongly limited the formation of water-stable aggregates; their formation was quantified upon a wet-sieving procedure by Bucka et al. (2021).

Among the OM treatments, the necromass treatment led to the development of the most distinct prokaryotic community. It hosted the largest population with the lowest alpha diversity and a clearly distinct beta diversity (Figures 1 and 4, Tables 1 and 2). This can be well explained by the composition of the added OM types. The necromass of *Bacillus subtilis* contains relatively few different OC compounds, including primarily proteins, nucleic acids, lipids, polysaccharides, and peptidoglycan (Neidhardt, 1996). POM and sPOM, in contrast, provide a broader range of OC compounds, consisting among others of cellulose, hemicellulose, lignin, starch, proteins, amino acids, sugars, nucleotides, waxes, and pigments (Paul, 2007). The larger diversity of OC compounds supported a more diverse prokaryotic community than necromass. The larger population size in the presence of necromass than with POM or sPOM indicates that the bacteria were more efficient in metabolizing microbial-derived OM than POM or sPOM. This is in line with the observation of Bucka et al. (2021), who saw a relative increase in the fungal population over the bacterial population in the two POM treatments compared to the necromass treatment, based on PLFA analysis. Thus, fungi contributed more to the degradation of POM and sPOM than to necromass degradation in comparison to the prokaryotes. Similar observations were, for example, made in forest soil, where fungi assimilated more carbon from plant-derived biomass than from microbial necromass, related to the metabolic capabilities of fungi and bacteria (López-Mondéjar et al., 2018, 2020). Most of the components of the bacterial necromass are relatively labile molecules, which can be rapidly metabolized by fast-growing bacteria and can even be used as direct precursors to build up biomass. They are consequently favorable for bacterial growth and provide high carbon use efficiency, whereas the more diverse OC compounds of plant litter support a microbial community with more diverse functions. Thus, bacteria can contribute more efficiently to the conversion of microbial necromass in soil than to plant biomass degradation. Consequently, the role of bacteria in early aggregate formation and stabilization is more efficiently supported by necromass, whereas fungi contribute to this process with support of plant-derived OM.

We also observed differences between the sPOM and POM treatments, that is, in dependence on OM particle size. Besides community-compositional differences, population size was clearly reduced in the POM compared to the sPOM treatment, though only in the clay and loam treatment and not in the sand treatment (Figure 1). These differences can in part be explained by a relative increase in the fungal population compared to the bacterial one (Bucka et al., 2021), indicating that fungi were even more competitive when large particles of OM were available as substrate compared to fine POM. Moreover, differences in the chemical composition of the OM materials have likely contributed to the differences in abundance and community composition. Analysis of the C:N ratio of the OM materials by Bucka et al. (2021) revealed a slightly higher C:N ratio in POM than sPOM, despite the identical origin. This shift resulted from size fractionation when preparing the sPOM. The stoichiometry of a substrate affects bacterial community development, whereby bacteria generally require a lower C:N ratio compared to fungi (Bending et al., 2002; Wan et al., 2015; Waring et al., 2013). Thus, the further increase in the fungal to bacterial ratio from sPOM to POM was probably the consequence of a slightly different chemical composition along with a further increase in the C:N ratio of the substrate.

The different particle size of POM versus sPOM had likely an even stronger impact on the prokaryotic community composition and abundance than the differences in chemical composition (Figures 1 and 4). Having larger POM particles will slow down the degradation process, as there is less surface that can be attacked by the microbes. The retarded degradation process was evident from higher OC contents in soils of the POM treatment compared to sPOM at the end of the incubation period, along with lower respiratory CO_2 release and less OC leaching in the POM treatment (Bucka et al., 2021). In the presence of larger POM particles, the degradation process will become more

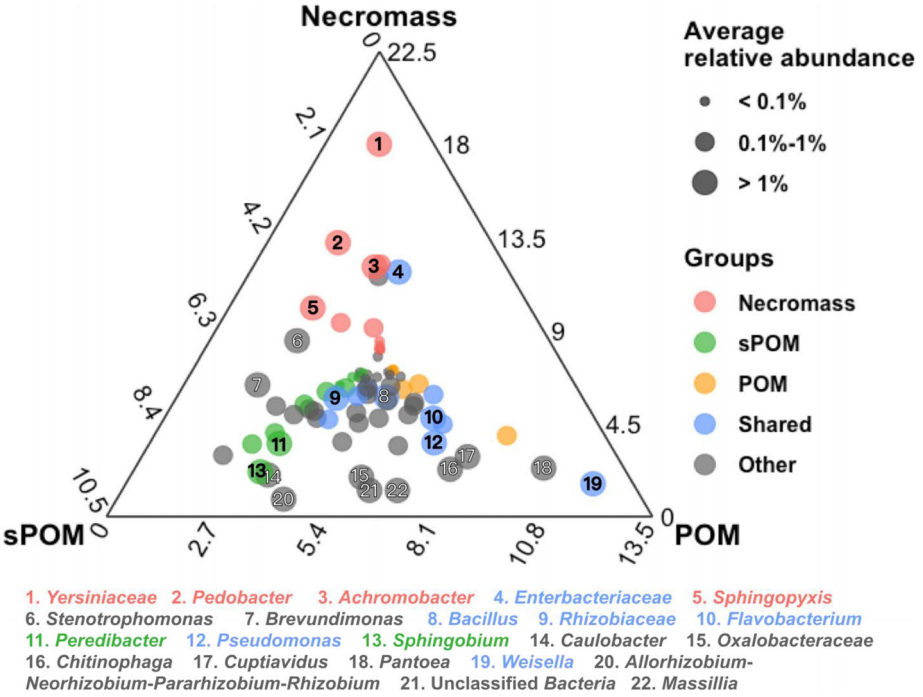

FIGURE 5 Abundant bacterial genera with significant differences in relative abundance in the OM treatments. Differences were analyzed by analysis of compositions of microbiomes with bias correction (ANCOM-BC) and are reported for significantly differentially abundant genera with 0.1% relative abundance at $p < 0.05$. The axes of the triangle denote the average relative abundance of the genera in the corresponding OM treatments. The coordinates of each genus are correlated to the relative abundance of the genus in the three OM treatments. The size of each point reflects the average relative abundance of a genus across all three OM treatments. The color code indicates significant enrichment in a specific OM treatment. Genera denoted as "other" were enriched in two treatments compared to the third one and "Shared" genera did not have a significant difference in relative abundance in an OM treatment. The most abundant genera (average relative abundance >1%) are numbered and names are listed below the plot. The identity of all enriched genera is listed in Table 2.

asynchronous compared to the degradation of small, more uniform POM particles. This may have contributed to the larger heterogeneity we observed in prokaryotic community composition in the POM treatment than with sPOM and necromass as substrate (Figure 4). Moreover, community assembly upon degradation of larger particles may include more random processes and priority effects, leading to more heterogenous communities; that is, the degradation process of individual POM particles may be initiated by different microbial taxa in different locations of the soil matrix, leading to variation in community development over time in dependence on the initiation of the process. However, this did not go along with an increase in prokaryotic diversity in the POM treatment compared to sPOM (Figure 3).

4.2 | Influence of texture on prokaryotic communities during early-stage aggregation

The influence of texture on prokaryotic community structure and abundance was less prominent than that of the OM treatments (Figure 1, Table 1). Texture-related changes were most evident within each of the three OM treatments and most pronounced in community composition (Table 1), while differences in abundance were not consistent in the different OM treatments (Figure 1) and differences in diversity were not observed (Figure 3). In large agreement with these findings, the ratio between fungi and bacteria, analyzed based on marker PLFAs, did not show a consistent response to texture in the different OM treatments (Bucka et al., 2021). Most evident were consistent changes in the POM treatment, which reflects the natural situation best when plant debris are introduced into soil. In this treatment, the qPCR data indicated that larger sized prokaryotic communities developed with increasingly coarser texture. Likewise, the respiration rate became increasingly higher in the POM treatments with increasingly coarser texture (Bucka et al., 2021), thus pointing toward a stronger support of bacterial growth in coarser-textured soils. Similarly, previous studies reported that soils with a coarser texture or lower soil clay content support soil bacterial communities of higher abundance (or biomass) and diversity (Naveed et al., 2016; Obayomi et al., 2021; Xia et al., 2020), though this is not a consistent finding (Sleutel et al., 2012; Yokobe et al., 2022). Texture appears to act interactively with other soil properties on bacterial growth (Seaton et al., 2020), leading to different outcomes in different studies. Based on the results of this study, the availability and type of OM appear to play a crucial role, either directly as substrate or indirectly by modulating aggregation and therewith microbial habitats.

Differences in experimental approaches between studies with the aim to study effects of texture on the microbiota have probably also contributed to heterogenous responses of microbial communities to variation in texture. Here, we varied texture by changing the ratios

of differently sized quartz grains, but we did not change the absolute amount of other minerals (i.e., illite, montmorillonite, and goethite), which provide reactive surfaces. In contrast to quartz grains, clay particles like illite and montmorillonite or iron (hydro)oxides like goethite are well known to interact specifically with bacteria due to their surface characteristics, therewith providing an explanation for the rather weak effects we observed in response to texture in this study. Montmorillonite is known to provide bacteria water on the surface and to maintain the pH for sustained growth (Stotzky, 1986). Illite and goethite have been reported to support the development of distinct bacterial communities in soil (Vieira et al., 2020), and soils with higher clay content were claimed to provide more or in some other studies less microhabitats (Obayomi et al., 2021). Goethite is further known to puncture bacterial cells during aggregation processes (Krause et al., 2019). By keeping the amount of these components constant between treatments, we modulated interactions between microbes and these reactive surface particles less than in other studies and therewith likely reduced the impact of texture.

Besides direct mineral–microbe interaction effects, texture can influence microbial colonization indirectly due to differences in the early aggregation process. Bucka et al. (2021) observed weaker aggregate stability in the sandy loam soil compared to clay loam in the presence of POM, which may lead to habitat heterogeneities. However, based on our moderate community compositional differences, aggregate traits defining microbial habitats were not highly relevant in our artificial soils. This may become different upon aggregate aging, as Olagoke et al. (2022) and De Gryze et al. (2006) pointed out that texture probably affects aggregation more strongly at later stages of the aggregate lifetime, being more relevant for stabilization than for formation. This aspect deserves further attention in future studies.

Another property of the artificial soils that was modulated by texture and aggregation and therewith likely relevant for the observed changes in prokaryotic community composition and abundance was water availability. Most pronounced in our incubations was a consistent increase in water content in the POM treatment (from 21 vol-% in sandy loam to 39 vol-% in clay loam), water-filled pore space (from 40 to 64 vol-%), and particle surface area being covered with OM as well as an increasing number of fine particles as published by Bucka et al. (2021). Thus, in the presence of POM as substrate, bacterial growth was best supported in the sandy loam, where the water-filled pore space was lowest and fewer but lager pores were observed. As small pores are known to limit nutrient supply and therewith survival (Keiluweit et al., 2017), they may have restricted the bacterial development in the clay loam.

4.3 | Prokaryotic communities showed different carbon acquisition strategies in dependence on OM types

The clear differences we observed in prokaryotic community composition (Figures 4 and 5) and respiration data (Bucka et al., 2021) between the necromass and (s)POM treatments demonstrate the relevance of OM type for microbial community formation. This is well in line with a recent conceptualization of microbial OM cycling in soil, in which microorganisms are categorized into four groups of ecological strategists based on their carbon acquisition strategies, including 1° decomposers, which degrade complex plant detritus; 2° decomposers, which degrade microbial necromass; passive consumers, which profit primarily from dissolved OC compounds; and predators, which live on living microbial biomass (Morrissey et al., 2023). With our setup, we disentangled the 1° and 2° decomposers by the POM versus necromass treatments. Some bacterial taxa were promoted by necromass, for example, *Pedopacter*, *Sphingopyxis*, *Luteimonas*, or *Devosia*, while others were characteristic in POM and/or sPOM treatments, such as *Sphingobium*, *Duganella*, *Rhizobium*, or *Massilia*. Also characteristic for POM/sPOM was *Chitinophaga*, a taxon able to degrade chitin (Sangkhobol & Skerman, 1981). It has possibly profited from fungal biomass that developed more strongly in the POM/sPOM treatments than in the necromass treatment (Bucka et al., 2021). Similarly, *Myxococcus* and *Peredibacter* had higher relative abundances in sPOM than in the other two treatments (Figure 5, Table 2). These genera have a predatory life style (Davidov & Jurkevitch, 2004; Muñoz-Dorado et al., 2016) and represent therewith the predators in the concept of Morrissey et al. (2023). *Duganella*, which was most enriched in the POM treatment, is known to produce lignin-degrading enzymes (Cretoiu et al., 2013) and to establish close cell–cell communication mechanisms for intra- and interspecies communication (Haack et al., 2016), indicating that an interconnected community is working together, especially on POM degradation.

A couple of taxa that were specifically enriched in the POM and/or sPOM treatments compared to the necromass treatment are known for degrading plant-derived OM in soil and are at the same time known as plant-associated bacteria. They may have been introduced with the hay particles, which represented the POM. These include *Azospirillum* (Table 2), which is a plant growth-promoting bacterium known for its capability to fix atmospheric nitrogen (Cassán et al., 2020). Members of the genera *Duganella*, *Pseudorhodoferax*, *Microvirga*, *Peredibacter*, and *Pantoea* and strains of the *Allorhizobium–Neorhizobium–Pararhizobium–Rhizobium* group have been reported as bacterial endophytes promoting plant growth (Campisano et al., 2017; Chimwamurombe et al., 2016; Jiménez-Gómez et al., 2019). Similarly, *Massilia*, which dominated in sPOM and POM treatments, can proliferate rapidly when attached to the plant surface (Cretoiu et al., 2013). These taxa in the POM/sPOM treatment may thus be remnants of the introduced OM. If not well adapted to survive in soil, they will decline in population size over time and contribute to the necromass pool.

Taxa that were abundantly detected in all three treatments included primarily copiotrophic bacteria, especially of the classes *Bacilli*, *Alphaproteobacteria*, and *Gammaproteobacteria*. Many of them are well known to be involved in OM degradation in soil, most prominently represented by *Bacillus* and *Pseudomonas*. Further examples are *Cohnella* and *Paenibacillus*, for example, known to be involved in straw degradation (Maarastawi et al., 2019), *Bosea*, active in cellulose and complex lignocellulose decomposition (Houfani et al., 2017), or *Sphingomonas* and *Caulobacter*, which degrade plenty of complex

organic compounds (Asaf et al., 2020; Wilhelm, 2018). They all have profited from the rich availability of OM in the incubations. In case of *Bacillus*, we cannot fully exclude that the high relative abundance in the necromass treatment was resulting from the added necromass itself, as it was derived from a *Bacillus* culture. However, we detected this taxon with comparable relative abundance in the POM and sPOM treatments, indicating that it can indeed develop a population size as observed in the necromass treatment.

4.4 | Bacterial contribution to soil aggregation

In the chronological order of aggregate formation, organic gluing agents derived from microbes are needed to initiate the aggregation process (Amelung et al., 2023). Members of most genera that were prominently present in all three OM treatments (Table 2) have the potential to secrete EPSs, including *Bacillus*, *Pseudomonas* (Roberson & Firestone, 1992), *Weissella* (Fusco et al., 2015; Teixeira et al., 2021), *Flavobacteria* (Zhang et al., 2015), *Rhizobiaceae* (Becker & Pühler, 1998), *Enterobacteriaceae* (Hua et al., 2010), *Sphingomonas* (Koutinas et al., 2019), *Paenibacillus* (Grady et al., 2016), *Bosea* (Lu et al., 2017), *Stenotrophomonas* (Caesar-TonThat et al., 2013), *Pedobacter* (Sharma, Kumar, et al., 2021), and *Sphingopyxis* (Sharma, Khurana, et al., 2021). EPS is known as important gluing agent for soil aggregates (Totsche et al., 2018). It associates with soil mineral particles by surface adsorption, connecting different minerals, OM particles, and microorganisms, thus enhancing soil aggregation (Costa et al., 2018). Besides, members of the genus *Luteimonas*, abundant in the necromass group, are able to produce bioemulsifiers, which play an important role in biofilm formation and might therewith influence the aggregation process (Franzetti et al., 2011), whereas members of *Achromobacter*, also abundant in the necromass group, were reported to secrete gum, thereby possibly stabilizing soil aggregation (Swaby, 1949). Functional redundancy in traits such as EPS production seems to ensure the contribution of microorganisms to aggregate formation despite variation in community structure, for example, when modulated by available OM types.

Despite this functional redundancy, a particular mass increase in microaggregates was observed in the necromass treatment, compared to the sPOM and POM treatments (Bucka et al., 2021). This may not only have been the consequence of the high prokaryotic abundance (Figure 1), but also of the added necromass itself. Soil aggregation is also supported by necromass, which encrusts with clay-sized particles and can stabilize soil microaggregates (Oades & Waters, 1991). Bacterial cell walls and their residues associate with small microaggregates or clay particles (Miltner et al., 2009) and serve as aggregate nucleus (Totsche et al., 2018). Taken together, the microbial population derived from the inoculum has likely supported aggregation in all OM treatments by gluing agents, while the necromass has additionally contributed to this in the respective treatment. In analogy to necromass, specific POM components have likely also supported aggregation to some extent (Besnard et al., 1996; Bucka et al., 2019).

5 | CONCLUSIONS

We observed that OM type and size exerted stronger effects on the developing prokaryotic community than soil texture. Texture-related effects resulting from direct mineral–microbe interactions were of little relevance here, because we modulated sand grain size rather than amount of minerals with reactive surfaces. Incubations with bacterial necromass led to the largest prokaryotic populations, whereas POM and sPOM supported better the fungal population as well as prokaryotic communities of higher diversity. Despite these differences, microaggregation occurred as long as OM was available, though it was more intense in the presence of necromass than in the POM treatments, likely related to the larger prokaryotic population that developed and supported initial aggregation steps by providing gluing agents. Functional redundancy in the microbiota regarding the formation of gluing agents has likely contributed to securing initial aggregate formation regardless of the available OM type. The OM itself has probably additionally contributed to the process in all OM treatments. Disentangling the relevance of these different processes needs to be addressed in future studies. As we studied the effects of necromass and POM in independent setups, we were able to shed light into the two microbial processes acting during initial aggregation. Plant-derived POM leads to the formation of microbial biomass by 1° degraders, which contribute to necromass buildup and formation of gluing agents. Both gluing agents and necromass therewith support aggregate formation in a first instance. Necromass buildup in turn supports a less complex but metabolically very efficient bacteria-dominated community of 2° degraders, which are likewise capable to produce gluing agents and therewith contribute to soil aggregation processes, possibly more effectively than the 1° degraders, which may in turn may be present in higher abundance in soil. The relative importance of these different ecological strategists to aggregate formation and stabilization in natural soils needs to be further elucidated.

ACKNOWLEDGMENTS

This study was financially supported by the *Deutsche Forschungsgemeinschaft* (*DFG*) within the framework of the *Research Unit 2179* entitled "*MAD Soil—Microaggregates: Formation and turnover of the structural building blocks of soils*" (*No. 276973576*). We would like to thank *Dr. Danh Biesgen*, *Dr. Katharina Frindte*, and *Merle Noschinski-Reetz* for technical support and valuable discussions.

Open access funding enabled and organized by Projekt DEAL.

DATA AVAILABILITY STATEMENT

The data that support the findings of this study are openly available in the National Center for Biotechnology Information (NCBI) at https://www.ncbi.nlm.nih.gov/bioproject/?term=PRJNA938122 (reference number: PRJNA938122).

ORCID

Franziska Bucka https://orcid.org/0000-0003-3922-8136
Claudia Knief https://orcid.org/0000-0001-5259-2675

REFERENCES

Amelung, W., Meyer, N., Rodionov, A., Knief, C., Aehnelt, M., Bauke, S. L., Biesgen, D., Dultz, S., Guggenberger, G., Jaber, M., Klumpp, E., Kögel-Knabner, I., Nischwitz, V., Schweizer, S. A., Wu, B., Totsche, K. U., & Lehndorff, E. (2023). Process sequence of soil aggregate formation disentangled through multi-isotope labelling. *Geoderma*, *429*, 116226. https://doi.org/10.1016/J.GEODERMA.2022.116226

Asaf, S., Numan, M., Khan, A. L., & Al-Harrasi, A. (2020). *Sphingomonas*: From diversity and genomics to functional role in environmental remediation and plant growth. *Critical Reviews in Biotechnology*, *40*(2), 138–152.

Becker, A., & Pühler, A. (1998). Production of exopolysaccharides. In H. P. Spaink, A. Kondorosi, & P. J. J. Hooykaas (Eds.), *The Rhizobiaceae* (pp. 97–118). Kluwer Academic.

Becker, M., Hellmann, M., & Knief, C. (2022). Spatio-temporal variation in the root-associated microbiota of orchard-grown apple trees. *Environmental Microbiome*, *17*, 31. https://doi.org/10.1186/s40793-022-00427-z

Bending, G. D., Turner, M. K., & Jones, J. E. (2002). Interactions between crop residue and soil organic matter quality and the functional diversity of soil microbial communities. *Soil Biology and Biochemistry*, *34*(8), 1073–1082.

Besnard, E., Chenu, C., Balesdent, J., Puget, P., & Arrouays, D. (1996). Fate of particulate organic matter in soil aggregates during cultivation. *European Journal of Soil Science*, *47*(4), 495–503.

Biesgen, D., Frindte, K., Maarastawi, S., & Knief, C. (2020). Clay content modulates differences in bacterial community structure in soil aggregates of different size. *Geoderma*, *376*, 114544. https://doi.org/10.1016/J.GEODERMA.2020.114544

Bolyen, E., Rideout, J. R., Dillon, M. R., Bokulich, N. A., Abnet, C. C., Al-Ghalith, G. A., Alexander, H., Alm, E. J., Arumugam, M., Asnicar, F., Bai, Y., Bisanz, J. E., Bittinger, K., Brejnrod, A., Brislawn, C. J., Brown, C. T., Callahan, B. J., Caraballo-Rodríguez, A. M., Chase, J., … Caporaso, J. G. (2019). Reproducible, interactive, scalable and extensible microbiome data science using QIIME 2. *Nature Biotechnology*, *37*(8), 852–857.

Bronick, C. J., & Lal, R. (2005). Soil structure and management: A review. *Geoderma*, *124*(1–2), 3–22.

Bucka, F. B., Felde, V. J., Peth, S., & Kögel-Knabner, I. (2021). Disentangling the effects of OM quality and soil texture on microbially mediated structure formation in artificial model soils. *Geoderma*, *403*, 115213. https://doi.org/10.1016/J.GEODERMA.2021.115213

Bucka, F. B., Kölbl, A., Uteau, D., Peth, S., & Kögel-Knabner, I. (2019). Organic matter input determines structure development and aggregate formation in artificial soils. *Geoderma*, *354*, 113881. https://doi.org/10.1016/J.GEODERMA.2019.113881

Buckeridge, K. M., Creamer, C., & Whitaker, J. (2022). Deconstructing the microbial necromass continuum to inform soil carbon sequestration. *Functional Ecology*, *36*(6), 1396–1410.

Caesar-TonThat, T. C., Espeland, E., Caesar, A. J., Sainju, U. M., Lartey, R. T., & Gaskin, J. F. (2013). Effects of *Agaricus lilaceps* fairy rings on soil aggregation and microbial community structure in relation to growth stimulation of western wheatgrass (*Pascopyrum smithii*) in Eastern Montana rangeland. *Microbial Ecology*, *66*, 120–131.

Campisano, A., Albanese, D., Yousaf, S., Pancher, M., Donati, C., & Pertot, I. (2017). Temperature drives the assembly of endophytic communities' seasonal succession. *Environmental Microbiology*, *19*(8), 3353–3364.

Cassán, F., Coniglio, A., López, G., Molina, R., Nievas, S., de Carlan, C. L. N., Donadio, F., Torres, D., Rosas, S., Pedrosa, F. O., de Souza, E., Zorita, M. D., de-Bashan, L., & Mora, V. (2020). Everything you must know about *Azospirillum* and its impact on agriculture and beyond. *Biology and Fertility of Soils*, *56*, 461–479.

Chao, A. (1984). Nonparametric estimation of the number of classes in a population. *Scandinavian Journal of Statistics*, *11*(4), 265–270.

Chimwamurombe, P. M., Grönemeyer, J. L., & Reinhold-Hurek, B. (2016). Isolation and characterization of culturable seed-associated bacterial endophytes from gnotobiotically grown Marama bean seedlings. *FEMS Microbiology Ecology*, *92*(6), fiw083. https://doi.org/10.1093/femsec/fiw083

Costa, O. Y., Raaijmakers, J. M., & Kuramae, E. E. (2018). Microbial extracellular polymeric substances: Ecological function and impact on soil aggregation. *Frontiers in Microbiology*, *9*, 1636. https://doi.org/10.3389/FMICB.2018.01636/BIBTEX

Cretoiu, M. S., Korthals, G. W., Visser, J. H., & van Elsas, J. D. (2013). Chitin amendment increases soil suppressiveness toward plant pathogens and modulates the actinobacterial and oxalobacteraceal communities in an experimental agricultural field. *Applied and Environmental Microbiology*, *79*(17), 5291–5301.

Davidov, Y., & Jurkevitch, E. (2004). Diversity and evolution of *Bdellovibrio*-and-like organisms (BALOs), reclassification of *Bacteriovorax starrii* as *Peredibacter starrii* gen. nov., comb. nov., and description of the *Bacteriovorax-Peredibacter* clade as *Bacteriovoracaceae* fam. nov. *International Journal of Systematic and Evolutionary Microbiology*, *54*(5), 1439–1452.

De Gryze, S., Jassogne, L., Bossuyt, H., Six, J., & Merckx, R. (2006). Water repellence and soil aggregate dynamics in a loamy grassland soil as affected by texture. *European Journal of Soil Science*, *57*(2), 235–246.

Franzetti, A., Gandolfi, I., Bertolini, V., Raimondi, C., Piscitello, M., Papacchini, M., & Bestetti, G. (2011). Phylogenetic characterization of bioemulsifier-producing bacteria. *International Biodeterioration & Biodegradation*, *65*(7), 1095–1099.

Frindte, K., Pape, R., Werner, K., Löffler, J., & Knief, C. (2019). Temperature and soil moisture control microbial community composition in an arctic–alpine ecosystem along elevational and micro-topographic gradients. *The ISME Journal*, *13*(8), 2031–2043.

Frindte, K., Zoche, S. A., & Knief, C. (2020). Development of a distinct microbial community upon first season crop change in soils of long-term managed maize and rice fields. *Frontiers in Microbiology*, *11*, 588198. https://doi.org/10.3389/FMICB.2020.588198/BIBTEX

Fusco, V., Quero, G. M., Cho, G. S., Kabisch, J., Meske, D., Neve, H., Bockelmann, W., & Franz, C. M. A. P. (2015). The genus *Weissella*: Taxonomy, ecology and biotechnological potential. *Frontiers in Microbiology*, *6*, 155. https://doi.org/10.3389/FMICB.2015.00155/BIBTEX

Grady, E. N., MacDonald, J., Liu, L., Richman, A., & Yuan, Z. C. (2016). Current knowledge and perspectives of *Paenibacillus*: A review. *Microbial Cell Factories*, *15*, 1.

Haack, F. S., Poehlein, A., Kröger, C., Voigt, C. A., Piepenbring, M., Bode, H. B., Daniel, R., Schäfer, W., & Streit, W. R. (2016). Molecular keys to the *Janthinobacterium* and *Duganella* spp. Interaction with the plant pathogen *Fusarium graminearum*. *Frontiers in Microbiology*, *7*, 1668. https://doi.org/10.3389/FMICB.2016.01668/BIBTEX

Houfani, A. A., Větrovský, T., Baldrian, P., & Benallaoua, S. (2017). Efficient screening of potential cellulases and hemicellulases produced by *Bosea* sp. FBZP−16 using the combination of enzyme assays and genome analysis. *World Journal of Microbiology and Biotechnology*, *33*, 29.

Hu, Y., Zheng, Q., Noll, L., Zhang, S., & Wanek, W. (2020). Direct measurement of the in situ decomposition of microbial-derived soil organic matter. *Soil Biology and Biochemistry*, *141*, 107660. https://doi.org/10.1016/j.soilbio.2019.107660

Hua, X., Wang, J., Wu, Z., Zhang, H., Li, H., Xing, X., & Liu, Z. (2010). A salt tolerant *Enterobacter cloacae* mutant for bioaugmentation of petroleum- and salt-contaminated soil. *Biochemical Engineering Journal*, *49*(2), 201–206.

Huang, P. M., Wang, M. K., & Chiu, C. Y. (2005). Soil mineral–organic matter–microbe interactions: Impacts on biogeochemical processes and biodiversity in soils. *Pedobiologia*, *49*(6), 609–635.

Jiménez-Gómez, A., Saati-Santamaría, Z., Igual, J. M., Rivas, R., Mateos, P. F., & García-Fraile, P. (2019). Genome insights into the novel species *Microvirga brassicacearum*, a rapeseed endophyte with biotechnological potential. *Microorganisms*, *7*(9), 354. https://doi.org/10.3390/microorganisms7090354

Keiluweit, M., Wanzek, T., Kleber, M., Nico, P., & Fendorf, S. (2017). Anaerobic microsites have an unaccounted role in soil carbon stabilization. *Nature Communications*, *8*(1), 1771. https://doi.org/10.1038/s41467–017–01406–6

Koutinas, M., Vasquez, M. I., Nicolaou, E., Pashali, P., Kyriakou, E., Loizou, E., Papadaki, A., Koutinas, A. A., & Vyrides, I. (2019). Biodegradation and toxicity of emerging contaminants: Isolation of an exopolysaccharide-producing *Sphingomonas* sp. for ionic liquids bioremediation. *Journal of Hazardous Materials*, *365*, 88–96.

Krause, L., Biesgen, D., Treder, A., Schweizer, S. A., Klumpp, E., Knief, C., & Siebers, N. (2019). Initial microaggregate formation: Association of microorganisms to montmorillonite-goethite aggregates under wetting and drying cycles. *Geoderma*, *351*, 250–260.

Lehmann, J., Kinyangi, J., & Solomon, D. (2007). Organic matter stabilization in soil microaggregates: Implications from spatial heterogeneity of organic carbon contents and carbon forms. *Biogeochemistry*, *85*(1), 45–57.

Lehndorff, E., Rodionov, A., Plümer, L., Rottmann, P., Spiering, B., Dultz, S., & Amelung, W. (2021). Spatial organization of soil microaggregates. *Geoderma*, *386*, 114915. https://doi.org/10.1016/J.GEODERMA.2020.114915

Liang, C., Amelung, W., Lehmann, J., & Kästner, M. (2019). Quantitative assessment of microbial necromass contribution to soil organic matter. *Global Change Biology*, *25*(11), 3578–3590.

Lin, H., & Peddada, S. D. (2020). Analysis of compositions of microbiomes with bias correction. *Nature Communications*, *11*, 3514. https://doi.org/10.1038/s41467–020–17041–7

López-Mondéjar, R., Brabcová, V., Štursová, M., Davidová, A., Jansa, J., Cajthaml, T., & Baldrian, P. (2018). Decomposer food web in a deciduous forest shows high share of generalist microorganisms and importance of microbial biomass recycling. *The ISME Journal*, *12*(7), 1768–1778.

López-Mondéjar, R., Tláskal, V., Větrovský, T., Štursová, M., Toscan, R., Nunes da Rocha, U., & Baldrian, P. (2020). Metagenomics and stable isotope probing reveal the complementary contribution of fungal and bacterial communities in the recycling of dead biomass in forest soil. *Soil Biology and Biochemistry*, *148*, 107875. https://doi.org/10.1016/J.SOILBIO.2020.107875

Lu, Y., Zhang, X., Feng, L., Yang, G., Zheng, Z., Liu, J., & Mu, J. (2017). Optimization of continuous-flow solid-phase denitrification via coupling carriers in enhancing simultaneous removal of nitrogen and organics for agricultural runoff purification. *Biodegradation*, *28*(4), 275–285.

Maarastawi, S. A., Frindte, K., Bodelier, P. L. E., & Knief, C. (2019). Rice straw serves as additional carbon source for rhizosphere microorganisms and reduces root exudate consumption. *Soil Biology and Biochemistry*, *135*, 235–238.

Miltner, A., Kindler, R., Knicker, H., Richnow, H. H., & Kästner, M. (2009). Fate of microbial biomass-derived amino acids in soil and their contribution to soil organic matter. *Organic Geochemistry*, *40*(9), 978–985.

Morrissey, E. M., Kane, J., Tripathi, B. M., Rion, M. S. I., Hungate, B. A., Franklin, R., Walter, C., Sulman, B., & Brzostek, E. (2023). Carbon acquisition ecological strategies to connect soil microbial biodiversity and carbon cycling. *Soil Biology and Biochemistry*, *177*, 108893. https://doi.org/10.1016/J.SOILBIO.2022.108893

Muñoz-Dorado, J., Marcos-Torres, F. J., García-Bravo, E., Moraleda-Muñoz, A., & Pérez, J. (2016). Myxobacteria: Moving, killing, feeding, and surviving together. *Frontiers in Microbiology*, *7*, 781. https://doi.org/10.3389/FMICB.2016.00781/BIBTEX

Naveed, M., Herath, L., Moldrup, P., Arthur, E., Nicolaisen, M., Norgaard, T., Ferré, T. P. A., & de Jonge, L. W. (2016). Spatial variability of microbial richness and diversity and relationships with soil organic carbon, texture and structure across an agricultural field. *Applied Soil Ecology*, *103*, 44–55.

Neidhardt, F. C. (1996). *Escherichia coli and Salmonella: Cellular and molecular biology*. ASM Press. https://books.google.de/books?id=CJK3XwAACAAJ

Oades, J. M., & Waters, A. G. (1991). Aggregate hierarchy in soils. *Soil Research*, *29*(6), 815–828.

Obayomi, O., Seyoum, M. M., Ghazaryan, L., Tebbe, C. C., Murase, J., Bernstein, N., & Gillor, O. (2021). Soil texture and properties rather than irrigation water type shape the diversity and composition of soil microbial communities. *Applied Soil Ecology*, *161*, 103834.

Olagoke, F. K., Bettermann, A., Nguyen, P. T. B., Redmile-Gordon, M., Babin, D., Smalla, K., Nesme, J., Sørensen, S. J., Kalbitz, K., & Vogel, C. (2022). Importance of substrate quality and clay content on microbial extracellular polymeric substances production and aggregate stability in soils. *Biology and Fertility of Soils*, *58*(4), 435–457.

Paul, E. A. (2007). Soil microbiology, ecology, and biochemistry in perspective. In E. A. Paul (Ed.), *Soil microbiology, ecology and biochemistry* (pp. 3–24). Academic Press.

Pielou, E. C. (1966). The measurement of diversity in different types of biological collections. *Journal of Theoretical Biology*, *13*, 131–144.

Pronk, G. J., Heister, K., Ding, G. C., Smalla, K., & Kögel-Knabner, I. (2012). Development of biogeochemical interfaces in an artificial soil incubation experiment; aggregation and formation of organo-mineral associations. *Geoderma*, *189*, 585–594.

Rillig, M. C., Muller, L. A., & Lehmann, A. (2017). Soil aggregates as massively concurrent evolutionary incubators. *The ISME Journal*, *11*(9), 1943–1948.

Roberson, E. B., & Firestone, M. K. (1992). Relationship between desiccation and exopolysaccharide production in a soil *Pseudomonas* sp. *Applied and Environmental Microbiology*, *58*(4), 1284–1291.

Sangkhobol, V., & Skerman, V. B. D. (1981). Chitinophaga, a new genus of chitinolytic myxobacteria. *International Journal of Systematic and Evolutionary Microbiology*, *31*(3), 285–293.

Seaton, F. M., George, P. B., Lebron, I., Jones, D. L., Creer, S., & Robinson, D. A. (2020). Soil textural heterogeneity impacts bacterial but not fungal diversity. *Soil Biology and Biochemistry*, *144*, 107766. https://doi.org/10.1016/j.soilbio.2020.107766

Shannon, C. E. (1948). A mathematical theory of communication. *The Bell System Technical Journal*, *27*(3), 379–423.

Sharma, M., Khurana, H., Singh, D. N., & Negi, R. K. (2021). The genus *Sphingopyxis*: Systematics, ecology, and bioremediation potential—A review. *Journal of Environmental Management*, *280*, 111744. https://doi.org/10.1016/j.jenvman.2020.111744

Sharma, P., Kumar, T., Yadav, M., Gill, S. S., & Chauhan, N. S. (2021). Plant-microbe interactions for the sustainable agriculture and food security. *Plant Gene*, *28*, 100325. https://doi.org/10.1016/j.plgene.2021.100325

Sleutel, S., Bouckaert, L., Buchan, D., Van Loo, D., Cornelis, W. M., & Sanga, H. G. (2012). Manipulation of the soil pore and microbial community structure in soil mesocosm incubation studies. *Soil Biology and Biochemistry*, *45*, 40–48.

Stotzky, G. (1986). Influence of soil mineral colloids on metabolic processes, growth, adhesion, and ecology of microbes and viruses. *Interactions of Soil Minerals with Natural Organics and Microbes*, *17*, 305–428.

Swaby, R. J. (1949). The relationship between micro-organisms and soil aggregation. *Microbiology*, *3*(2), 236–254.

Teixeira, C. G., Fusieger, A., Milião, G. L., Martins, E., Drider, D., Nero, L. A., & de Carvalho, A. F. (2021). *Weissella*: An emerging bacterium with promising health benefits. *Probiotics and Antimicrobial Proteins*, *13*(4), 915–925.

Totsche, K. U., Amelung, W., Gerzabek, M. H., Guggenberger, G., Klumpp, E., Knief, C., Lehndorff, E., Mikutta, R., Peth, S., Prechtel, A., Ray, N., & Kö Gel-Knabner, I. (2018). Microaggregates in soils. *Journal of Plant Nutrition and Soil Science*, *181*(1), 104–136.

Vieira, S., Sikorski, J., Gebala, A., Boeddinghaus, R. S., Marhan, S., Rennert, T., Kandeler, E., & Overmann, J. (2020). Bacterial colonization of minerals in grassland soils is selective and highly dynamic. *Environmental Microbiology*, *22*, 917–933.

Wan, X., Huang, Z., He, Z., Yu, Z., Wang, M., Davis, M. R., & Yang, Y. (2015). Soil C:N ratio is the major determinant of soil microbial community structure

in subtropical coniferous and broadleaf forest plantations. *Plant and Soil*, *387*, 103–116.

Wang, X., Zhang, W., Zhou, F., Liu, Y., He, H., & Zhang, X. (2020). Distinct regulation of microbial processes in the immobilization of labile carbon in different soils. *Soil Biology and Biochemistry*, *142*, 107723. https://doi.org/10.1016/j.soilbio.2020.107723

Waring, B. G., Averill, C., & Hawkes, C. V. (2013). Differences in fungal and bacterial physiology alter soil carbon and nitrogen cycling: Insights from meta-analysis and theoretical models. *Ecology Letters*, *16*(7), 887–894.

Wilhelm, R. C. (2018). Following the terrestrial tracks of *Caulobacter*-redefining the ecology of a reputed aquatic oligotroph. *The ISME Journal*, *12*(12), 3025–3037.

Xia, Q., Rufty, T., & Shi, W. (2020). Soil microbial diversity and composition: Links to soil texture and associated properties. *Soil Biology and Biochemistry*, *149*, 107953.

Yokobe, T., Hyodo, F., Tateno, R., & Tokuchi, N. (2022). Soil mineral fraction influences the bacterial abundance: Evidence from a mineral and plant materials incubation study. *Biogeochemistry*, *161*(3), 273–287.

Zhang, Z., Chen, Y., Wang, R., Cai, R., Fu, Y., & Jiao, N. (2015). The fate of marine bacterial exopolysaccharide in natural marine microbial communities. *PLoS ONE*, *10*(11), e0142690. https://doi.org/10.1371/journal.pone.0142690

SUPPORTING INFORMATION

Additional supporting information can be found online in the Supporting Information section at the end of this article.

How to cite this article: Yao, T., Bucka, F., Kögel-Knabner, I., & Knief, C. (2024). Organic matter type and soil texture shape prokaryotic communities during early-stage soil structure formation. *Journal of Plant Nutrition and Soil Science*, *187*, 89–103. https://doi.org/10.1002/jpln.202300142